BOREAL ENVIRONMENT RESEARCH 19 (suppl. B): 108–121 © 2014
ISSN 1239-6095 (print) ISSN 1797-2469 (online) Helsinki 30 September 2014

Urban nitrous-oxide fluxes measured using the eddy-covariance technique in Helsinki, Finland

Leena Järvi[1)], Annika Nordbo[1)], Üllar Rannik[1)], Sami Haapanala[1)], Anu Riikonen[2)], Ivan Mammarella[1)], Mari Pihlatie[1)] and Timo Vesala[1)]

[1)] *Department of Physics, P.O. Box 48, FI-00014 University of Helsinki, Finland*
[2)] *Department of Forest Ecology, P.O. Box 27, FI-00014 University of Helsinki, Finland*

Received 5 Dec. 2013, final version received 12 Mar. 2014, accepted 12 Mar. 2014

Järvi, L., Nordbo, A., Rannik, Ü., Haapanala, S., Riikonen, A., Mammarella, I., Pihlatie, M. & Vesala, T. 2014: Urban nitrous-oxide fluxes measured using the eddy-covariance technique in Helsinki, Finland. *Boreal Env. Res.* 19 (suppl. B): 108–121.

Using the eddy covariance technique, nitrous oxide (N_2O) fluxes were measured at the semi-urban SMEAR III station in Helsinki, Finland, between 21 June and 27 November 2012. The measurement period covered a seasonal change from summer to autumn allowing us to examine variations in the N_2O fluxes by season. Also, varying land cover around the measurement site enabled us to study the effects of different urban land covers on the N_2O exchange. Overall, the measurement surroundings acted as a source of N_2O with a median and quartile deviation for the campaign of 1.7 ± 2.0 μmol m^{-2} h^{-1}. The net emissions were slightly higher from the direction of green areas than from the direction of roads under heavy traffic indicating that vegetation cannot be neglected in the urban N_2O exchange studies. No seasonal change in the N_2O flux during the measurement campaign was found.

Introduction

Measured by its impact on radiative forcing, nitrous oxide (N_2O) is the third important anthropogenic greenhouse gas in the atmosphere after carbon dioxide (CO_2) and methane (IPCC 2013). Besides its warming effect on our climate (10% that of CO_2), N_2O also plays an important role in the chemical depletion of stratospheric ozone (Ravinshakara *et al*. 2009). Anthropogenic activities, including agriculture (16%), biomass burning (5%) and energy/industry (4%), account for approximately 40% of the global sources of N_2O (Fowler *et al*. 2009). The rest of N_2O is emitted mainly from oceans and soil. Due to anthropogenic activities, urban areas may act as hotspots of N_2O emissions not only from energy production and traffic, but also from managed vegetation. N_2O emissions from vegetated surfaces are mainly related to the amount of nitrogen in soil and the microbial production of N_2O via nitrification and denitrification processes. Thus, nitrogen-rich fertilizers play a key role in N_2O emissions in managed green areas (Jones *et al*. 2011, Butterbach-Bahl *et al*. 2013). Soils can also act as a sink for N_2O due to N_2O consumption in denitrification or nitrifier denitrification processes under varying environmental conditions (Chapuis-Lardy *et al*. 2007).

In Helsinki, the three most important sources of N_2O are energy production (43%), traffic (29%) and agriculture (13%) (Carney *et al*.

Editor in charge of this article: Veli-Matti Kerminen

2009). These values, as well as greenhouse gas emission estimates in general, are calculated at an annual scale from national inventories. These inventories, however, lack information about the spatial and temporal variability of the emissions and sinks of the compounds inside a city, and typically ignore the effect of urban green areas. Variability of the exchange at a neighbourhood scale is important especially from the point of view of urban planning and climate mitigation.

The eddy covariance (EC) technique is a direct micrometeorological method to measure the exchange of greenhouse gases and other atmospheric pollutants between the surface and the atmosphere at a local scale, and it has successfully been used in various ecosystems for multiple compounds (e.g. Fowler *et al*. 2009, Aubinet *et al*. 2012). Only in the recent years, EC measurements of greenhouse gas emissions in urban areas have become popular, but the studies were mainly concentrated on CO_2 (e.g. Velasco and Roth 2010, Grimmond and Christen 2012). Studies have so far successfully compared these measurements with budget-based CO_2 net emission (e.g. Christen *et al*. 2011, Nordbo *et al*. 2012b), showing that the technique can successfully be used to follow the exchange of greenhouse gases in urban areas. To date, only one study has reported urban N_2O fluxes from the city of Edinburgh, Scotland, over one month (Famulari *et al*. 2010). Thus, little is known about the spatial variability of N_2O exchange at a city scale as well as its temporal variability both at the diurnal and seasonal scales. Urban areas are a mixture of built and green areas and therefore not only anthropogenic emissions, but also the effect of vegetation needs to be understood.

In this study, we report the results of an N_2O flux EC measurement campaign carried out at the semi-urban SMEAR III (Station for Measuring Ecosystem–Atmosphere Relations, Järvi *et al*. 2009c) Kumpula site in Helsinki between June and November 2012. The measurement site is located at a high latitude and therefore is characterised by distinct seasons with varying vegetation activity. The surroundings of the flux-measurement tower fall into three surface-cover categories: roads under heavy traffic, buildings or green areas. This allowed us to examine the impact of different surface-cover types on the exchange of N_2O. Temporal changes in the N_2O flux at the diurnal and seasonal scales were also examined, and correlations between net fluxes and environmental factors affecting the exchange were studied.

Measurement site and measurements

Measurement site

The measurements were carried out at the semi-urban measurement station SMEAR III Kumpula site (Fig. 1a) located 4 km NE from the Helsinki city centre (Järvi *et al*. 2009c). The eddy covariance measurements were performed from the top level of a 31-m-high lattice tower (60°12.17´N, 24°57.671´E) located on a hill, 26 m a.s.l. and 19–21 m above the surrounding terrain. The area around the tower can be divided into three surface cover sectors: built, road and vegetation, each representing the typical surface cover of the area (Vesala *et al*. 2008). The built sector in the northern direction (320°–40°) is dominated by university campus buildings and the Finnish Meteorological Institute (mean height 20 m) in the vicinity of the measurement tower. In this direction the observations can occasionally be in the roughness sublayer and therefore should be considered with caution. One of the main roads leading to Helsinki city centre passes through the road sector (40°–180°) with the closest distance between the road and the tower being 150 m. The area in-between is covered by deciduous forest with mainly birch, Norway maple, aspen, goat willow and bird cherry (Vesala *et al*. 2008). On the road, a typical workday traffic rate is around 44 000 vehicles per day (Lilleberg and Hellman 2011), and the vehicles have been found to be the main source of CO_2 and aerosol particle emissions in the area (Järvi *et al*. 2012, Ripamonti *et al*. 2013). In the vegetation sector (180°–320°), most of the surface is covered by green areas in the Kumpula Botanic Garden and in the City Allotment Garden. Fertilization and irrigation routines differ largely between the gardens. In the allotment garden, cultivation is only allowed between May and September, industrial fertilizers are banned and only manual irrigation is

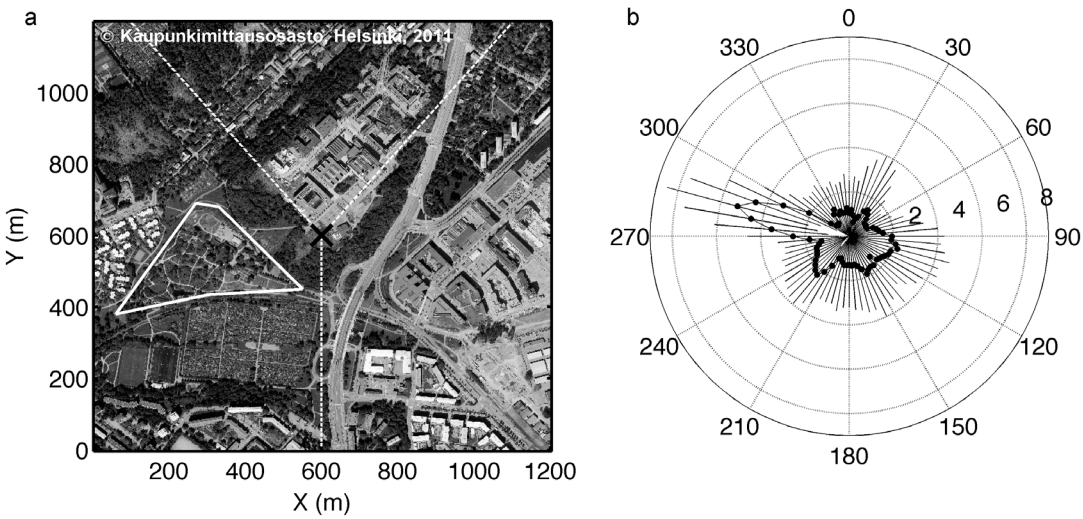

Fig. 1. (**a**) Aerial photograph of the study site, where the flux tower is marked with black cross, the Kumpula Botanic Garden with white solid lines, and the different surface cover sectors with white dashed lines. (**b**) The median N_2O fluxes (μmol m^{-2} h^{-1}) for 20° wind direction sectors calculated with 5° interval. Zero degree corresponds to north. The whiskers show the quartile deviations.

allowed. In the botanical garden, on the other hand, industrial fertilizers to keep the non-indigenous vegetation species alive are regularly used. In addition, when the botanic garden was rebuilt in 2006–2009, most of the plants and grass were planted on composted sewage sludge (L. Schulman, Finnish Museum of Natural History, University of Helsinki, pers. comm.), leaving lots of nitrogen (N)-rich organic material in the soil. Indigenous soils around the measurement tower are predominantly rock and till, and till or clay in low-lying areas, where both gardens are located.

Measurement setup

The eddy covariance setup to measure the N_2O flux consisted of an ultrasonic anemometer (USA-1, Metek GmbH, Germany) and a TDL spectrometer (Tunable diode laser, TGA-100A, Campbell Scientific Inc., USA) to measure the N_2O mixing ratio. TDL comprises a single-mode diode laser controlled by current and temperature, and it is tuned to an infrared N_2O absorption band. The laser itself is installed in a liquid nitrogen dewar. A concentration measurement is obtained by passing the infrared laser beam through an absorption tube to the sample and reference cells. Reference gas of 2200 ppm N_2O was drawn through the reference cell at the same temperature and pressure as the sample air in the sample cell. The TDL was calibrated twice during the measurement campaign and liquid nitrogen was added to the dewar bi-weekly. The conditions of the laser and the instrument were checked weekly, and the laser was adjusted twice during the campaign due to the line shift. The TDL spectrometer has successfully been used to measure the N_2O fluxes in various ecosystems (e.g. Wienhold *et al*. 1994, Pihlatie *et al*. 2005b, Rinne *et al*. 2005).

Complementary CO_2 flux measurements were performed with a closed-path infrared gas analyzer (LI-7000, LI-COR, Lincoln, Nebraska, USA) using the same anemometer and partly the same inlet and tube. The anemometer was located 31 m above ground on a horizontal boom south-west from the tower. The air inlet of the gas analysers was situated 0.13 m below the anemometer centre. A 40-m-long steel tube with the inner diameter of 8 mm leaded to the CO_2 analyser from where the air was further drawn to the TDL through a 10-m-long steel tube with the inner diameter of 4 mm. The flow rates in the tubes were 20.2 and 17.2 l min^{-1}, respectively, to ensure turbulent flow, and the sampling line

was heated with a power of 16 W m^{-2} to avoid condensation of water vapour. The frequency of the measurements was 10 Hz and the raw data were stored for post-processing. The N_2O flux measurements carried out between 21 June and 27 November 2012, whereas the CO_2 flux is measured continuously.

Auxiliary measurements

The auxiliary measurements cover global radiation (CNR1, Kipp&Zonen, Delft, Netherlands) and air temperature (Platinum resistant thermometer, Pt-100, built in-house) measured from the top boom of the EC tower at the height of 31 m. In addition, precipitation was measured on the roof of a nearby building using a weighting rain gauge (Pluvio2, Ott Messtechnik GmbH, Germany). Soil volumetric water content at 10 cm depth was measured continuously at two sites (three points each) in a neighbourhood called Viikki, around 4 km east from the Kumpula site. The measurements were made from growing media (area not covered by impervious surfaces) of street trees using Theta-probes (ML2x, Delta T Devices Ltd., Cambridge, UK) (Riikonen *et al*. 2011). Despite the distance between the EC flux tower and the soil-moisture measurement site, the results are considered to be representative for the changes in soil moisture also at the Kumpula site.

Hourly traffic rates were measured online 4 km from the Kumpula site by the City of Helsinki Planning Department. Observations were made hourly outside the rush hours (06:00–09:00 LST, Local Standard Time = UTC + 2 hours), and four times an hour at other times. These rates were converted to correspond to the traffic rates on the road next to the measurement site (Järvi *et al*. 2012).

Data analysis and quality screening

Flux calculations

The 30-min N_2O fluxes were calculated from the raw data using the maximum covariance technique with a fixed lag-time window (e.g. Foken *et al*. 2012). Prior to the calculation of the final fluxes, raw data were de-spiked and linearly detrended, and a two-dimensional coordinate rotation was applied. The N_2O signal measured by the TDL was frequently dominated by a low-frequency signal drifting that previous studies have reported to be caused by the optical interference fringes. The drifting was suppressed by applying a high-pass autoregressive running mean filter with a time constant of 50 seconds before the flux calculations (e.g. Mammarella *et al*. 2010). As the sample air was dried prior to the analyser, and the measurement tube dampens the temperature fluctuations, no WPL correction was needed.

The N_2O fluxes (F_n) were corrected for losses at the high- and low-frequency ends of the co-spectra as follows:

$$\frac{F_n^m}{F_n} = \frac{\int_0^\infty \mathrm{TF_H}(f)\,\mathrm{TF_L}(f)\,C_{ws}(f)\,df}{\int_0^\infty C_{ws}(f)\,df}, \quad (1)$$

where F_n^m and F_n are the measured and un-attenuated N_2O fluxes (μmol m^{-2} h^{-1}), f is the natural frequency (Hz), $\mathrm{TF_H}$ and $\mathrm{TF_L}$ are the transfer functions describing high- and low frequency losses. Both transfer functions were calculated as the product of appropriate theoretical transfer functions as described in Moncrieff *et al*. (1997) and Rannik and Vesala (1999). $C_{ws}(f)$ is the site-specific temperature co-spectrum that is assumed to be un-attenuated. The stability dependency of $C_{ws}(f)$ was taken into account when correcting each 30-minute F_n values. The peak co-spectral frequencies were taken as the maxima of fits to the co-spectra, and they were further converted to a normalized form as

$$n_m = f_m(z - z_d)/U, \quad (2)$$

where z is the measurement height, z_d is the displacement height (Vesala *et al*. 2008), and U is the wind speed. The normalized peak frequency is expected to be constant in unstable conditions and depend on atmospheric stability (ζ) in stable conditions with the form

$$n_m = \alpha_1\left(1 + \alpha_2\zeta^{\alpha_3}\right), \quad (3)$$

where α_1, α_2, α_3 are fitting coefficients. Detailed

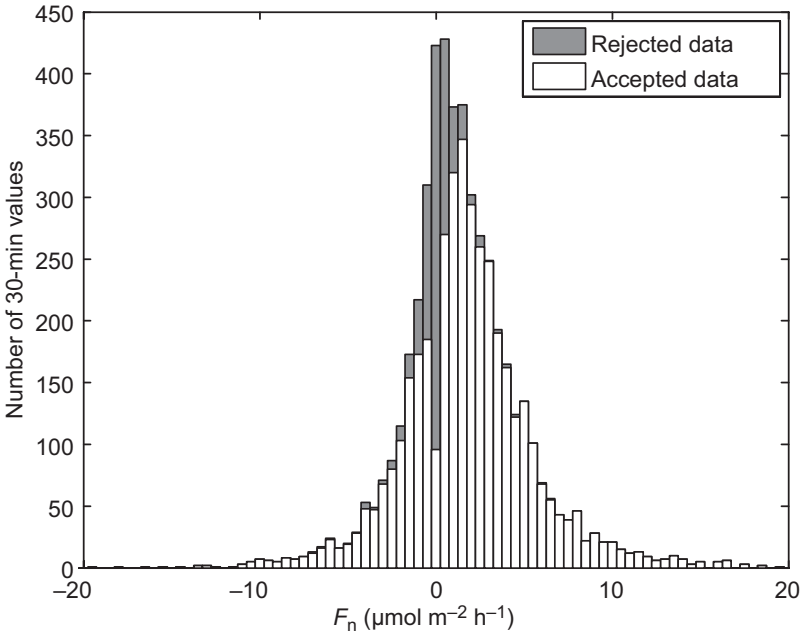

Fig. 2. Histogram of N_2O fluxes (F_n) before and after the quality screening.

description of the data handling of the CO_2 fluxes and spectral calculations is given in (Järvi *et al*. (2009a) and Nordbo *et al*. (2012a).

Flux quality screening

During the 160-day measurement campaign, 36% of the N_2O flux data were lost due to power and instrument failures. In October, 98% of data were missing due to a data logging malfunction. Additionally, obvious outliers were removed from the N_2O flux data (covering 0.1%), and data were omitted according to the stationarity test that ensures that the stationarity criteria required by the EC technique is met (Foken and Wichura 1996). Data were omitted if the 30-minute flux values deviated more than 100% from the average of 5-minute subsections, corresponding to quality flag six (Foken *et al*. 2004). The stationarity test removed 10.7% of the N_2O fluxes (Fig. 2). The test mainly removes small fluxes increasing the campaign average by 16%. Finally, 53% of the N_2O flux data were available for further analysis.

Besides the data quality assurance, the flux detection limit and random error can be used to describe the quality of the flux measurements. The detection limit gives the minimal flux level that the instrument is able to detect due to uncertainties arising from instrumental noise. It is defined as the standard deviation of the cross-correlation function far away from the peak, i.e., the maximum of the function, following Wienhold *et al*. (1994) with the modifications given in Nordbo *et al*. (2012a). The flux random error (Lenschow *et al*. 1994) gives the error due to a finite flux averaging time and it incorporates flux random error due to stochastic nature of turbulence as well as instrumental noise. Both the detection limit and the flux random error are converted to have units of covariance and normalized by the covariance values.

Results

Performance of the measurement setup

Quality of the measurements was assessed by inspecting the N_2O co-spectra. The median co-spectrum for unstable stratification follows a theoretical model (Kaimal *et al*. 1972) fairly well, with the exception of some deviation in the inertial sub-range (Fig. 3). In theory, white noise in the N_2O time series should not correlate with vertical wind speed and thus it should not be seen in a co-spectrum. Nevertheless, some deviation from the theoretical slope was found

for a limited frequency interval at normalised frequencies above five. As this deviation is outside the energy-containing range, irs impact on the flux will be small.

As expected, the co-spectral peak frequencies (n_m) are constant in unstable situations with values 0.10 ± 0.04 and 0.08 ± 0.04 for CO_2 and N_2O, respectively. On the other hand, a clear stability dependency of the N_2O peak frequency in the form $n_m = 0.08(1 + 3.0\zeta^{0.47})$ was found (Eq. 3). The first fitting coefficient α_1 corresponds to the constant value in unstable conditions. Both the unstable mean values and the stability dependency in stable conditions are close to those found for the fluxes of sensible and latent heat, CO_2 and aerosol particles at the same site (Vesala *et al*. 2008, Järvi *et al*. 2009b, 2009c).

The campaign median detection limit and the random error normalized with F_n were 0.53 ± 0.67 and 0.50 ± 0.60, respectively, where the errors are quartile deviations (also hereinafter). Thus, on average the flux is twice the minimum flux that can be measured with the instrumentation, and it can be concluded that the instrumentation was sensitive enough for the measurements of low fluxes in a semi-urban environment. The relative detection limit and random uncertainty of the N_2O flux are over two times higher than obtained for momentum, sensible and latent heat, and CO_2 fluxes at the same site during several years of measurements (Järvi *et al*. 2012, Nordbo *et al*. 2012a), and at an urban site in downtown Helsinki (Nordbo *et al*. 2013). The detection limit for N_2O fluxes from an agricultural soil has been determined to be 0.06–0.17 of the flux, which is 1/5 of that at our site (Wienhold *et al*. 1995).

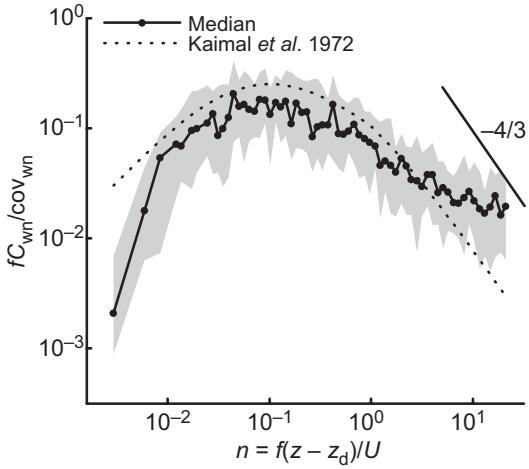

Fig. 3. Median N_2O flux co-spectrum (C_{wn}) multiplied by the natural frequency (f) and normalized with the covariance (cov_{wn}) (black line), quartile deviation (gray area) and model co-spectrum by Kaimal *et al.* (1972) (dashed line) as a function of normalized frequency n. Data were binned into 76 logarithmically evenly-spaced classes and only co-spectra with $F_n > 15$ μmol m^{-2} h^{-1} and unstable stratification were included (42 cases) in the plot.

Weather conditions

During the measurement campaign, a seasonal change from summer to autumn took place (Fig. 4). The daytime (10:00–14:00) daily median global radiation ranged from ~830 W m^{-2} to 5 W m^{-2} at the start and the end of the campaign, respectively, with the cloudy days clearly visible in the time series. Similarly, the daily air temperature was at its maximum 23 °C in late July and the lowest daily temperature (–6 °C) was measured in early November. Precipitation was evenly distributed along the measurement campaign, but some separate weeks without rain were registered in 8–15 August and 22 Oct–2 Nov. During the measurement campaign, the most dominant wind direction was the S-SW, i.e., the direction where the highest fraction of vegetation cover was located (Fig. 5).

F_n did not vary between summer and autumn. The maximum daily flux 7.2 μmol m^{-2} h^{-1} was found at the end of July. At the daily level, the surroundings acted as a source of N_2O with the exception in mid-August when slightly negative fluxes were measured (Fig. 4d).

Spatial and seasonal variability of N_2O fluxes

Median F_n ranged between 0.5 and 4.6 μmol m^{-2} h^{-1} with the highest upward fluxes from the direction 270°–290° (Fig. 1b). In this direction, the management area of the botanical garden as well as the newest part of the garden are located. These elevated fluxes can be explained by more intense fertilization, and thus more nitrogen rich soil, in the latter part of the

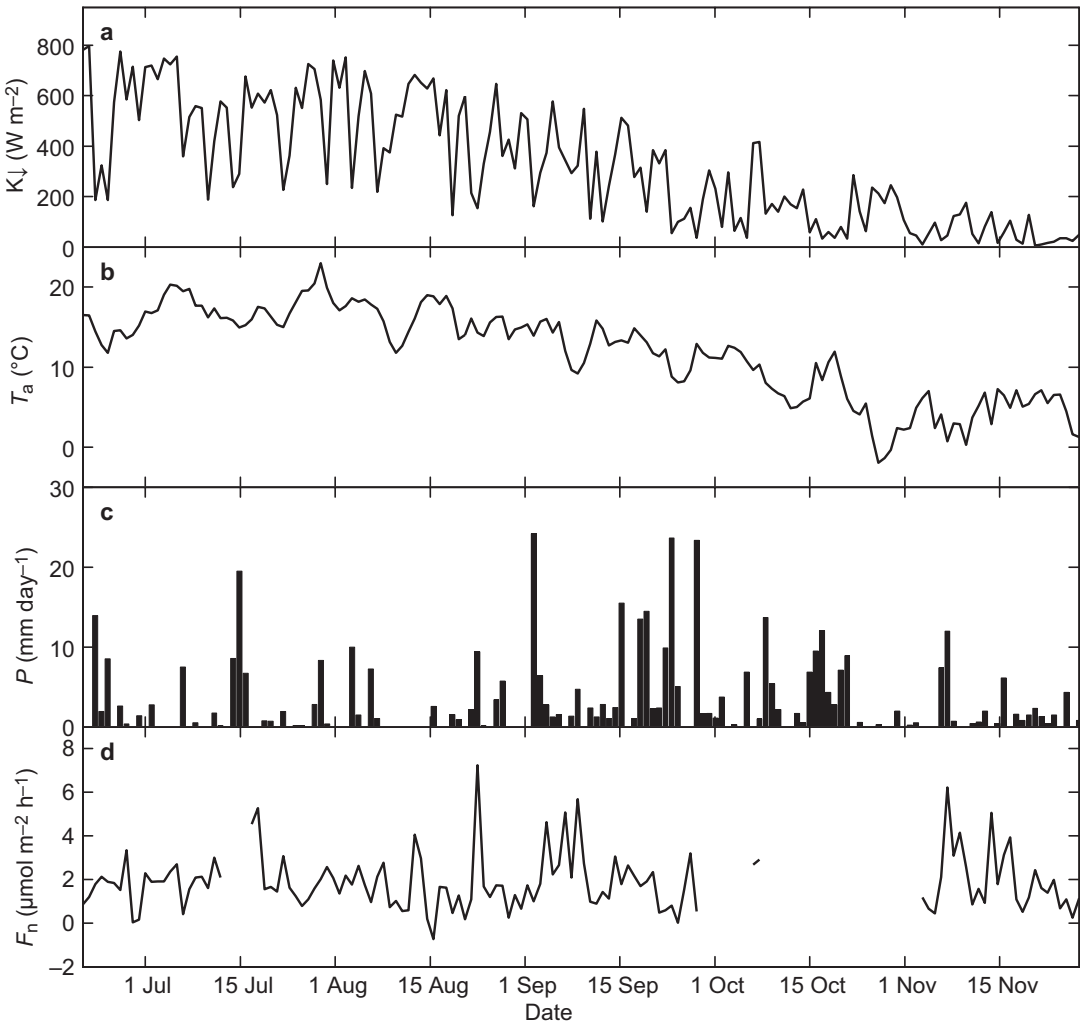

Fig. 4. Time series of daily mean (**a**) daytime (10:00–14:00) global radiation ($K\downarrow$), (**b**) air temperature (T_a), (**c**) precipitation (P), and (**d**) N_2O flux (F_n) at the SMEAR III Kumpula site during 21 June–27 Nov 2012.

garden as compared with that in the older part of the garden and the nearby allotments. Also point N_2O emissions from the management areas, including fertilization storage and greenhouses, cannot be neglected. From the other parts of the garden and from the allotments (180°–260°), the fluxes were between 1 and 2.5 μmol m^{-2} h^{-1}.

Another direction with elevated F_n was that of the road (80°–160°) where the fluxes reached 2.2 μmol m^{-2} h^{-1}. Also the CO_2 flux had a peak in that direction indicating the impact of traffic emissions on the N_2O signal (not shown). The lowest N_2O fluxes, on the other hand, were measured from the direction of the built sector (320°–20°) close to the measurement tower where both the amount of road traffic and vegetation are at their minima.

Based on the wind-direction dependence of F_n, it is reasonable to consider the different surface-cover sectors (built, road and vegetation) separately in further analysis. Excluding June, the highest N_2O emissions were recorded from the direction of the vegetation sector (Fig. 6). In June, only 9 days of data were available for analysis so the monthly median is not that representative. October was left empty due to the small amount of data caused by the instrument failure. The highest monthly emission, 2.3 μmol m^{-2} h^{-1},

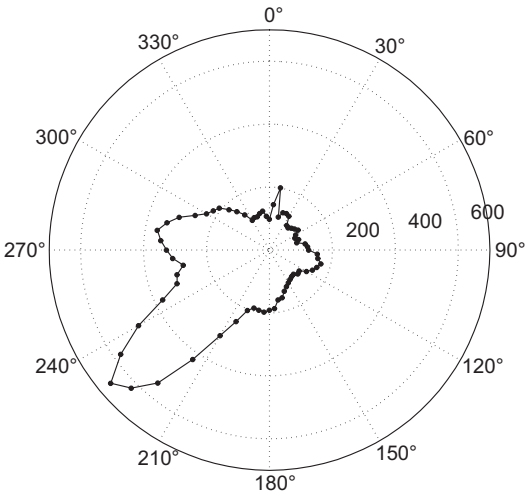

Fig. 5. The occurrence of 20° wind directions calculated for 5° interval; 0° corresponds to the north.

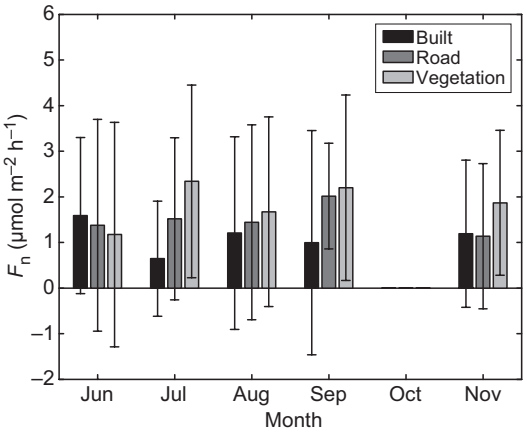

Fig. 6. Median N_2O fluxes (F_n) for the difference surface cover sectors (built, road and vegetation) in each month. Quartile deviations are shown with error bars.

was measured in July from the vegetation sector, and the lowest 0.6 μmol m^{-2} h^{-1} in same month from the built sector. When averaged over the whole measurement campaign, the median fluxes for vegetation, road and built areas were 2.0, 1.4 and 1.2 μmol m^{-2} h^{-1}, respectively (Table 1).

During the measurement campaign, F_n did not change seasonally (Fig. 4) despite the fact that there is more road traffic outside summer months in addition to the increasing need for heating in autumn. Generally in Helsinki, and also around the flux tower, most buildings use district heating, but some houses north of the flux tower may additionally use fireplaces. In summer, F_n is more affected by vegetation and soil whereas in autumn litter may have stimulated soil N_2O emissions (Pihlatie *et al*. 2007). Median F_n during the measurement campaign was 1.7 ± 2.0 μmol m^{-2} h^{-1}. The median net flux in Edinburgh in November was tenfold (11.7 μmol m^{-2} h^{-1}, Famulari *et al*. 2010) than measured at our site in the same month. This can be explained by the proximity of a dense downtown area to their flux tower, where there is likely more traffic than on the roads passing nearby our measurement site. Unfortunately, no other F_n values from urban areas using the same micrometeorological techniques have been reported and the impact of dense urban areas on the fluxes cannot be verified. Our median value is slightly smaller than obtained for agricultural sites, which can be explained by intensive nitrogen fertilization of agricultural soils leading to

Table 1. Monthly median daytime (10:00–14:00) global radiation ($K\downarrow$) and air temperature (T), monthly cumulative precipitation (P) and median N_2O fluxes (F_n) for each surface cover sector around the EC flux tower. Quartile deviations of F_n are shown for the campaign medians.

	Jun	Jul	Aug	Sep	Oct	Nov	Campaign
$K\downarrow$ (W m^{-2})	723	609	531	218	121	33	254
T (°C)	13.3	17.5	16.1	12.7	6.8	4.6	12.7
P (mm month^{-1})	90	63	47	175	100	65	540
F_n (μmol m^{-2} h^{-1})							
Built	1.59	0.64	1.20	0.99	–	1.19	1.18 ± 1.94
Road	1.38	1.52	1.44	2.01	–	1.14	1.41 ± 1.89
Veg	1.17	2.34	1.67	2.20	–	1.87	1.96 ± 1.87
All	1.30	1.93	1.53	2.11	–	1.63	1.70 ± 1.97

higher N_2O emissions (Table 2). As compared with that for more natural ecosystems, our value is slightly higher. On the other hand, around 100 times higher emissions were measured from a landfill in Helsinki using the same instrument (193 μmol m^{-2} h^{-1}; *see* Rinne *et al*. 2005).

Diurnal behaviour of the N_2O fluxes

As the flux tower was rarely downwind from the built sector (Fig. 5), lots of data for this direction are missing.

Although, F_n showed highly variable behaviour similarly to what was found by Famulari *et al*. (2010), but still a distinct diurnal cycles were seen both in the vegetation and road sectors (Fig. 7a). Downwind from these two directions, however, the behaviour was different indicating differences in sources/sinks. Using the Mann-Whitney *U*-test we found that the differences between the fluxes in these two surface-cover sectors were significant (U = 1980, p = 0.0109). In the vegetation sector, maximum F_n (3.9 μmol m^{-2} h^{-1}) was measured in the afternoon, whereas the nocturnal fluxes remained below 2 μmol m^{-2} h^{-1}. This indicates that the N_2O emissions were related to soil microbial activity, which in general increases with increasing soil temperature. Also, as the maximum F_n occurred at the same time with a maximum uptake of CO_2 (–7 μmol m^{-2} s^{-1}), emissions may also be related to the vegetation activity as N_2O can be emitted from trees via transpiration (Pihlatie *et al*. 2005a).

Slightly higher maximum F_n than that in the vegetation sector was measured for the road sector during daytime (4.2 μmol m^{-2} h^{-1}). F_n started to increase around 05:00 LST corresponding well with the start of the morning rush hour (Fig. 6c). At the same time, an increase was also seen in the CO_2 flux, F_c (Fig. 7b). The morning and rush-hour maxima of F_n were 3.5 μmol m^{-2} h^{-1} and 4.1 μmol m^{-2} h^{-1}, respectively, and they also coincided with the F_c maxima (9.7 and 10.4 μmol m^{-2} s^{-1}, respectively). Thus, F_n and F_c showed traffic-related similarity in the direction of the road under heavy traffic.

A linear regression between the median fluxes and traffic values showed a clear dependence of F_n on F_c (RMSE = 0.94 μmol m^{-2} h^{-1}, r = 0.59) and traffic rate (RMSE = 0.76 μmol m^{-2} h^{-1}, r = 0.76) (Fig. 8). The intercept of the latter regression equation (0.27 μmol m^{-2} h^{-1}; *see* Fig. 8b) can be considered to represent contributions from other sources than traffic to the N_2O signal, which in this direction is mainly vegetation in residential areas. This would correspond well with F_n measured in natural/agricultural ecosystems in Europe (Table 2).

Our diurnal peak fluxes were much lower than 32 μmol m^{-2} h^{-1} reported for Edinburgh in Famulari *et al*. (2010). In order to understand the differences, we drew a plot similar to their fig. 6b, where median F_n for the road sector were calculated for 200 vehicles per half-hour bins (Fig. 9). Fluxes increased with increasing vehicle numbers, but the maximum fluxes were found for the range 1200–1400 vehicles per 30 min not for the maximum traffic rates.

Table 2. Mean N_2O fluxes (F_n, μmol m^{-2} h^{-1}) measured using the eddy-covariance technique in different environments. Reference values were chosen according to the representativeness of ecosystems and environments.

Location	Site	Period	F_n	Reference
Helsinki, Finland	Landfill	Aug 2003	192.7*	Rinne *et al.* (2005)
Edinburgh, UK	Urban	Nov–Dec 2005	11.7**	Famulari *et al.* (2010)
Helsinki, Finland	Urban	Jun–Nov 2012	1.7**	This study
Harford, NY, USA	Agricultural	Jun–Jul 2008	2.8*	Molodovskaya *et al.* (2011)
Lägeren, Switzerland	Mixed forest	Oct–Nov 2005	0.8*	Eugster *et al.* (2007)
Easter Bush, UK	Grassland	Jan–Dec 2002	0.5**	Fletchard *et al.* (2007)
		Jan–Dec 2003	0.2**	
Lille Bøgeskov, Denmark	Beech forest floor	May–Jun 2005	0.4**	Pihlatie *et al.* (2005b)
Kalevansuo, Finland	Peatland forest	Apr–Jun 2007	0.3**	Mammarella *et al.* (2010)

* mean, ** median.

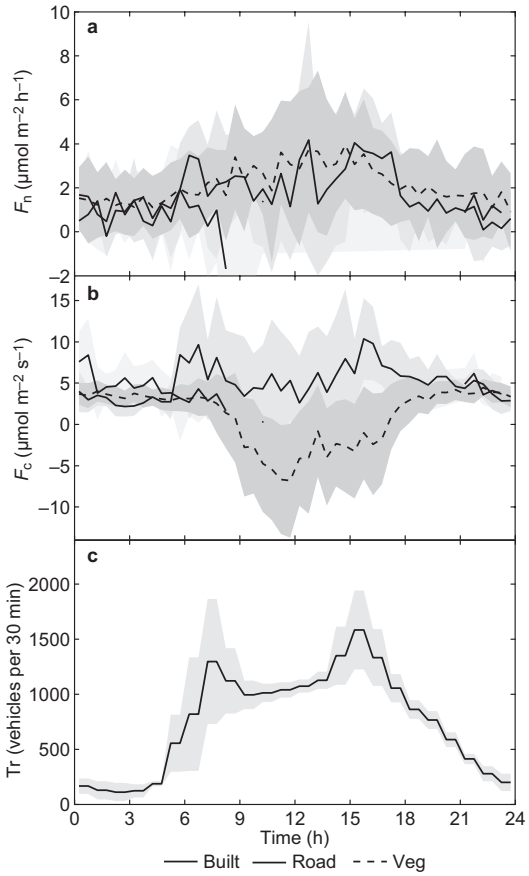

Fig. 7. Diurnal behaviour of the median (**a**) N_2O flux (F_n), (**b**) CO_2 flux (F_c), and (**c**) traffic rates (Tr) during the measurement campaign. Fluxes are shown for the built, road and vegetation sectors. The shaded areas show the quartile deviations. Only data when both F_n and F_c were available were considered and only half hours with more than 10 data points are shown in the plot. This way, only nocturnal data from the built surface cover sectors are plotted.

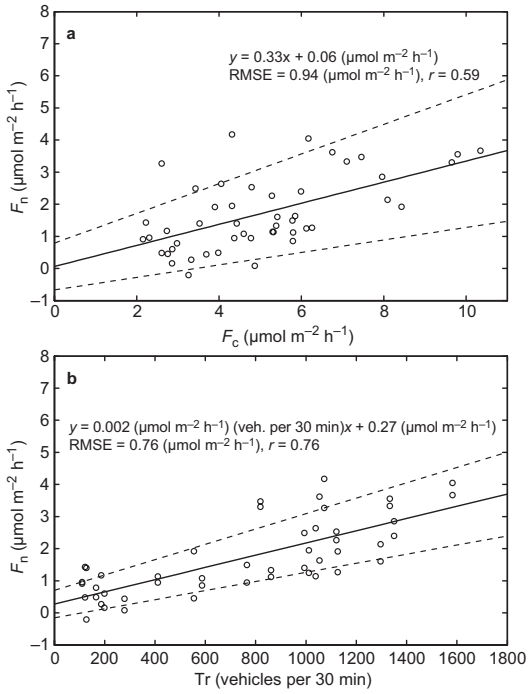

Fig. 8. Correlations between the median half-hour N_2O fluxes (F_n) and (**a**) CO_2 flux (F_c), and (**b**) traffic rate (Tr). The data correspond to the 48 data points representing the road sector in Fig. 6. The solid line is the linear regression and the dashed lines indicate the 95% confidence limits.

Similar behaviour was also found for particle fluxes at the site (Järvi *et al*. 2009b), and it is thought to be related to the amount of congestion, increased number of heavy-duty vehicles during the rush hours, and the enhanced mixing of the atmosphere as these traffic rates correspond to the daytime hours. The overall dependency in Helsinki and Edinburgh is qualitatively similar with increasing fluxes with higher traffic, but the flux magnitudes are systematically one order of magnitude smaller in Helsinki than in Edinburgh. Since in our case, the road next to the flux tower is known to be the main pollutant emitter in that direction, we assume that the different relationship in Edinburgh is caused by the downtown area where several roads with more traffic are located. Similarly to F_n, also F_c was found to be greater (three times in November) in Edinburgh than at our site in Helsinki (Nemitz *et al*. 2002).

N_2O emissions factors relative to CO_2 emissions

It is common to analyse the emission ratio (ER) of different air pollutants respective to F_c, as CO_2 is considered to be a good tracer for anthropogenic emissions (e.g. Järvi *et al*. 2009b, Famulari *et al*. 2010, Vogt *et al*. 2011). ER was thus calculated as a campaign median for the road sector yielding 6.4×10^{-5}. Obtained ER corresponds well with the annual value of 6.7×10^{-5} obtained from emission inventories for residential and

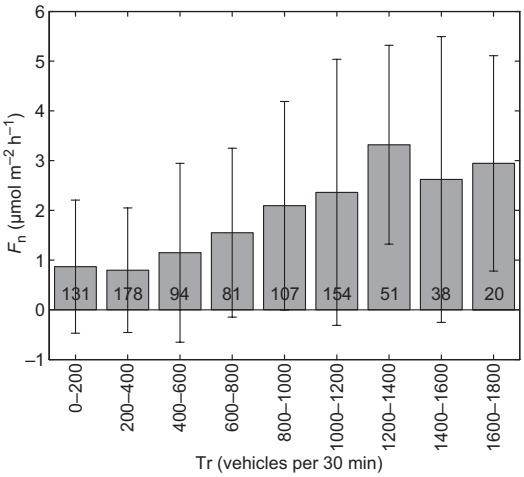

Fig. 9. Dependence of half-hourly N_2O fluxes (F_n) on local traffic rate (Tr) at the SMEAR III Kumpula road sector. Median values for bins of 200 vehicles per 30 min were calculated. Error bars show the quartile deviations and the numbers in the bars indicate how many half-hour data points were in each bin.

transport emissions in Helsinki (Carney *et al*. 2009). The emissions from the direction of the road can be considered to be mainly a combination of these two sources, but unfortunately it was not possible to determine their relative contributions, which causes discrepancy in the comparison of ER from inventories and EC measurements.

ER obtained from the measurements can be used as a proxy for annual N_2O emissions with the aid of annual CO_2 emissions from the road sector. Järvi *et al*. (2012) reported a five-year mean annual CO_2 emission of 3500 g C m^{-2} for the road sector, which would give 0.26 g N m^{-2} for annual N_2O emission. This value is only approximate as unfortunately we do not have information on how N_2O fluxes behave in winter and spring at our measurement site.

Impact of soil moisture on N_2O emissions

N_2O emissions from soils are known to be dependent on soil moisture and its changes as water affects the oxygen availability for soil microbes (e.g. Pihlatie *et al*. 2005b, Butterbach-Bahl *et al*. 2013). Therefore, we analysed our N_2O fluxes from the direction of the vegetation sector together with the average volumetric soil water content (θ_v, %; *see* Fig. 10). Wetting of the soil followed precipitation events well (e.g. on 15–17 July and 2 September) despite the 4-km distance between our site and the site where precipitation was measured. This proofs that these precipitation values can be used as a reference for soil moisture changes in Kumpula.

Most of the time, the increase and decrease in daily F_n followed the changes in soil moisture well (Fig. 10). Almost always an increase in soil moisture was followed by a peak in N_2O emissions. However, the correlation between the daily means did not exist (r = 0.08), but this could be expected as the vegetation around the flux tower is more intensively managed than at the soil-moisture measurement sites. However, the comparison suggests that also at urban sites the N_2O net fluxes are, to some degree, dependent on the soil moisture and not only on anthropogenic emissions. This implies that microbial activity in the soil and vegetation play an important role in N_2O emissions at urban sites. F_n were also compared with other meteorological variables, including air temperature and global radiation, but no dependency was found.

Conclusions

In Helsinki, an N_2O flux measurement campaign using the eddy-covariance technique was carried out in June–November 2012. The measurement period covered the seasonal change from summer to autumn allowing us to examine the seasonal variation in N_2O fluxes. Furthermore, the different surface-cover sectors around our flux tower allowed us to examine the effects of different urban land-covers on the measured fluxes.

Overall, the measurement surrounding was a source of N_2O with a median net flux of 1.7 ± 2.0 μmol m^{-2} h^{-1}. Higher fluxes were measured from the highly vegetated area (median = 2.0 μmol m^{-2} h^{-1}) than from the direction of road under heavy traffic (median = 1.4 μmol m^{-2} h^{-1}). The highest emissions were recorded from the new area of the Kumpula Botanic Garden, where the vegetation is more managed as compared

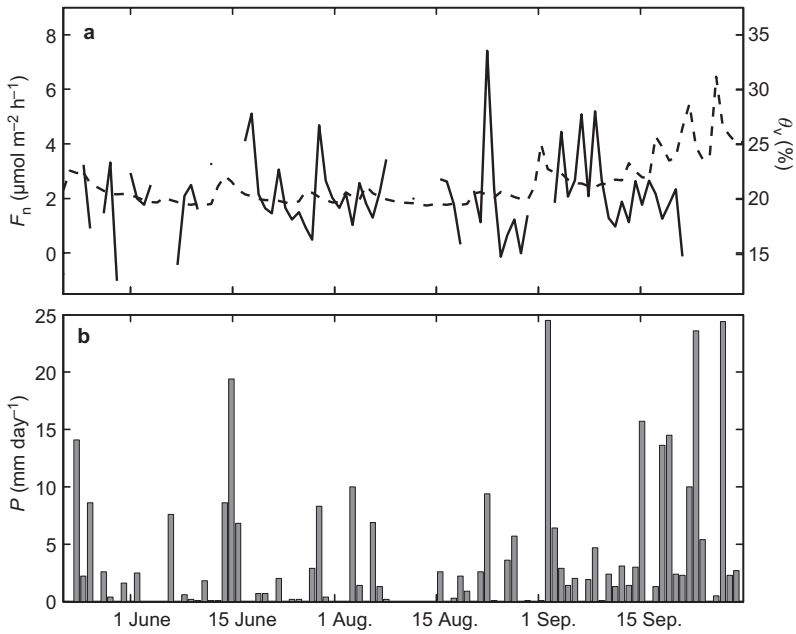

Fig. 10. Daily mean (**a**) N_2O flux (F_n) at the SMEAR III vegetation sector (solid line) and soil volumetric water content (dashed line) measured in Viikki (θ_v), and (**b**) precipitation (P) between 21 June and 31 September 2012.

to the other green areas around the flux tower. In the area of high fraction of vegetation, N_2O emissions seemed to be dependent on the soil moisture similarly to non-urban ecosystems. In the direction of the road, a clear effect of local traffic on the N_2O fluxes in a diurnal cycle was found and the correlation between the N_2O and CO_2 fluxes, and between the N_2O flux and traffic rate were high (0.59 and 0.76, respectively; *see* Fig. 8). Using the measurements, we also calculated emission ratios for the road sector (6.4×10^{-5}) that matched well with the ratios obtained from an inventory study. The N_2O fluxes did not show a seasonal behaviour during the autumn transformation.

The results suggest that the eddy-covariance technique can be used to measure the exchange of N_2O at our site, and that the impact of urban vegetation on the N_2O exchange. So far only two urban N_2O studies, including the current one, have been made. The three-fold difference in the values of F_n emphasizes the need for additional observations in urban areas that differ in their population density and degree of development. These are needed in order to draw general conclusions about N_2O exchange in urban areas and dependencies of the emissions on road traffic and vegetation.

Acknowledgements: This work was supported by the Academy of Finland (project nos. 138328, 1127756, and ICOS-Finland 263149), the Academy of Finland Centre of Excellence (project no. 1118615), the Nordic Center of Excellence DEFROST and the EU 7th framework project InGOS. We also thank Joonas Moilanen and Erkki Siivola for the instrument maintenance and Helsinki City Planning Department for the traffic rates.

References

Aubinet M., Vesala T. & Papale D. (eds.) 2012. *Eddy covariance: A practical guide to measurement and data analysis*. Springer Atmospheric Sciences, Springer, Dordrecht, Heidelberg, London, New York.

Butterbach-Bahl K., Baggs E.M., Dannenmann M., Kiese R. & Zechmeister-Boltenstern S. 2013. Nitrous oxide emissions from soils: how well do we understand the processes and their controls. *Phil. Trans. R. Soc. B* 368: 20130122, .

Chapuis-Lardy L., Wrage N., Metay A., Chotte J.L. & Bernoux M. 2007. Soils, a sink for N_2O: a review. *Glob. Change Biol.* 13: 1–17.

Carney S., Green N.W. & Read R. 2009. *Greenhouse gas emissions inventories for 18 European regions. EU CO_2 80/50 project stage 1: Inventory formation. The Greenhouse Gas Regional Inventory Protocol (GRIP)*. Centre for Urban and Regional Ecology School of Environment and Development, University of Manchester.

Christen A., Coops N.C., Crawford B.R., Kellett R., Liss K.N., Olchovski I., Tooke T.R., van der Laan M. & Voogt J.A. 2011. Validation of modeled carbon-diox-

ide emissions from an urban neighborhood with direct eddy-covariance measurements. *Atmos. Environ.* 45: 6057–6069.

Eugster W., Zeyer K., Zeeman M., Michna P., Zingg A., Buchmann N. & Emmenegger L. 2007. Methodical study of nitrous oxide eddy covariance measurements using quantum cascade laser spectrometery over a Swiss forest. *Biogeosciences* 4: 927–939.

Famulari D., Nemitz E., Di Marco C., Phillips G.J., Thomas R., House E. & Fowler D. 2010. Eddy-covariance measurements of nitrous oxide fluxes above a city. *Agric. For. Meteorol.* 150: 786–793.

Flechard C.R., Ambus P., Skiba U., Rees R.M., Hensen A., van Amstel A., van den Pol-van Dasselaar A., Soussana J.-F., Jones M., Clifton-Brown J., Raschi A., Horvath L., Neftel A., Jocher M., Ammann C., Leifeld J., Fuhrer J., Calanca P., Thalman E., Pilegaard K., Di Marco C., Campbell C., Nemitz E., Hargreaves K.J., Levy P.E., Ball B.C., Jones S.K., van de Bulk W.C.M., Groot T., Blom M., Domingues R., Kasper G., Allard V., Ceschia E., Cellier P., Laville P., Henault C., Bizouard F., Abdalla M., Williams M., Baronti S., Berretti F. & Grosz B. 2007. Effects of climate and management intensity on nitrous oxide emissions in grassland systems across Europe. *Agr. Ecosyst. Environ.* 121: 135–152.

Foken T. & Wichura B. 1996. Tools for quality assessment of surface-based flux measurements. *Agric. For. Meteorol.* 78: 83–105.

Foken T., Leuning R., Oncley S.R., Mauder M. & Aubinet M. 2012. Corrections and data quality control. In: Aubinet M., Vesala T. & Papale D. (eds.), *Eddy covariance: A practical quide to measurement and data analysis*, Springer Atmospheric Sciences, Springer, Dordrecht, Heidelberg, London, New York, pp. 85–131.

Foken T., Göckede M., Mauder M., Mahrt, L. Amiro B.D. & Munger J.W. 2004. Post-field data quality control. In: Lee X., Massman W. & Law B. (eds.), *Handbook of micrometeorology: a guide for surface flux measurement and analysis*, Kluwer, Dordrecht, pp. 181–208.

Fowler D., Pilegaard K., Sutton M.A, Ambus P., Raivonen M., Duyzer J., Fuzzi S., Schjoerring J.K., Granier J., Neftel A., Isaksen I.S.A., Laj P., Maione M., Monks P.S., Burkhardt J., Daemmgen U., Neirynck J., Personne E., Wichink-Kruit R., Butterbach-Bahl K., Flechard C., Tuovinen J.P., Coyle M., Gerosa G., Loubet B., Altimir N., Gruenhage L., Ammann C., Cieslik S., Paoletti E., Mikkelsen T.N., Ro-Poulsen H., Cellier P., Cape J.N., Horváth L., Loreto F., Niinemets Ü., Palmer P.I., Rinne J., Misztal P., Nemitz E., Nilsson D., Pryor S., Gallagher M.W., Vesala T., Skiba U., Brüggemann N., Zechmeister-Boltenstern S., Williams J., O'Dowd C., Facchni M.C., de Leeuw G., Flossman A., Chaumerliac N. & Erisman J.W. 2009. Review: atmospheric composition change: ecosystems–atmosphere interactions. *Atmos. Environ.* 43: 5193–5267.

Grimmond C.S.B. & Christen A. 2012. *The newsletter of FLUXNET* 5: 1–8.

IPCC 2013. *Working group 1 contribution to the IPCC 5th assessment report climate change: the physical basis*. Cambridge University Press, Cambridge, UK and New York, NY, USA.

Jones S.K., Famulari D., Di Marco C.F. Nemitz E., Skiba U.M., Rees R.M. & Sutton M.A. 2011. Nitrous oxide emissions from managed grassland: a comparison of eddy covariance and static chamber measurements. *Atmos. Meas. Tech.* 4: 2179–2194.

Järvi L., Nordbo A., Junninen H., Riikonen A., Moilanen J., Nikinmaa E. & Vesala T. 2012. Seasonal and annual variation of carbon dioxide surface fluxes in Helsinki, Finland, in 2006–2010. *Atmos. Chem. Phys.* 12: 8475–8489.

Järvi L., Mammarella I., Eugster W., Ibrom A., Siivola E., Dellwik E., Keronen P., Burba G. & Vesala T. 2009a. Comparison of net CO_2 fluxes measured with open- and closed-path infrared gas analyzers in an urban complex environment. *Boreal Env. Res.* 14: 499–514.

Järvi L., Rannik Ü., Mammarella I., Sogachev A., Aalto P.P., Keronen P., Siivola E., Kulmala M. & Vesala T. 2009b. Annual particle flux observations over a heterogeneous urban area. *Atmos. Chem. Phys.* 9: 7847–7856.

Järvi L., Hannuniemi H., Hussein T., Junninen H., Aalto P.P., Hillamo R., Mäkelä T., Keronen P., Siivola E., Vesala T. & Kulmala M. 2009c. The urban measurement station SMEAR III: Continuous monitoring of air pollution and surface-atmosphere interactions in Helsinki, Finland. *Boreal Env. Res.* 14 (suppl. A): 86–109.

Kaimal J.C., Izumi Y., Wyngaard J.C. & Cote R. 1972. Spectral characteristics of surface-layer turbulence. *Q. J. R. Meteorol. Soc.* 98: 563–589.

Lenschow D.H., Mann J. & Kristensen L. 1994. How long is long enough when measuring fluxes and other turbulence statistics? *J. Atmos. Ocean. Technol.* 11: 661–673.

Lilleberg I. & Hellman T. 2011. *Liikenteen kehitys Helsingissä vuonna 2011*. Helsinki City Planning Department 2011, 2.

Mammarella I., Werle P., Pihlatie M., Eugster W., Haapanala S., Kiese R., Markkanen T., Rannik Ü. & Vesala T. 2010. A case study of eddy covariance flux of N_2O measured within forest ecosystems: quality control and flux error analysis. *Biogeosciences* 7: 427–440.

Molodovskaya M., Warland J., Richards B.K., Öberg G. & Steenhuis T.S. 2011. Nitrous oxide from heterogeneous agricultural landscapes: source contribution analysis by eddy covariance and chambers. *Soil Sci. Sc. Am. J.* 75: 1829–1838.

Moncrieff J., Massheder J.M., de Bruin H., Elbers J., Friborg T., Heusinkveld B., Kabat P., Scott S., Soegaard H. & Verhoef A. 1997. A system to measure surface fluxes of momentum, sensible heat, water vapour and carbon dioxide. *J. Hyrdrol.* 188–189: 589–611.

Nemitz E., Hargreaves K.J., Mcdonald A.G., Dorsey J. & Fowler D. 2002. Micrometeorological measurements of the urban heat budget and CO_2 emissions on a city scale. *Environ. Sci. Techol.* 36: 3139–3146.

Nordbo A., Järvi L. & Vesala T. 2012a. Revised eddy covariance flux calculation methodologies — effect on urban energy balance. *Tellus* 64B, 18184, doi:10.3402/tellusb.v64i0.18184.

Nordbo A., Järvi L., Haapanala S., Wood C.R. & Vesala T. 2012b. Fraction of natural area as main predictor of net CO_2 emissions from cities. *Geophys. Res. Lett.* 39,

20802, doi:10.1029/2012GL053087.

Nordbo, A., Järvi, L., Haapanala, S., Moilanen, J. & Vesala, T. 2013. Intra-city variation in urban morphology and turbulence structure in Helsinki, Finland. *Boundary-Layer Meteorol*. 146: 469–496.

Pihlatie M., Ambus P., Rinne J., Pilegaard K. & Vesala T. 2005a. Plant-mediated nitrous oxide emissions from beech (*Fagus sylvatica*) leaves. *New Phytologist* 168: 93–98.

Pihlatie M., Pumpanen J., Rinne J., Ilvesniemi H., Simojoki A., Hari P. & Vesala T. 2007. Gas concentration driven fluxes of nitrous oxide and carbon dioxide in boreal forest soil. *Tellus* 59B: 458–469.

Pihlatie M., Rinne J., Ambus P., Pilegaard K., Dorsey J.R., Rannik Ü., Markkanen T., Launiainen S. & Vesala T. 2005b. Nitrous oxide emissions from a beech forest floor measured by eddy covariance and soil enclosure techniques. *Biogeosciences* 2: 377–387.

Rannik Ü. & Vesala T. 1999. Autoregressive filtering versus linear detrending in estimation of fluxes by the eddy covariance method. *Boundary-Layer Meteorol*. 91: 259–280.

Ravinshakara A.R., Daniel J.S. & Portmann R.W. 2009. Nitrous oxide (N_2O): the dominant ozone-depleting substance emitted in the 21st century. *Science* 326: 123–125.

Rinne J., Pihlatie M., Lohila A., Thum T., Aurela M., Tuovinen J.-P., Laurila T. & Vesala T. 2005. Nitrous oxide emissions from a municipal landfill. *Environ. Sci. Techonol*. 39: 7790–7793.

Riikonen A., Lindén L., Pulkkinen M. & Nikinmaa E. 2011. Post-transplant crown allometry and shoot growth of two species of street trees. *Urban For. Urban Greening* 10: 87–94.

Ripamonti G., Järvi L., Mølgaard M., Hussein T., Nordbo A. & Hämeri K. 2013. The effect of local sources on aerosol particle number size distribution, concentrations and fluxes in Helsinki, Finland. *Tellus* 65B, 19786, doi:10.3402/tellusb.v65i0.19786.

Velasco E. & Roth M. 2010. Cities as net sources of CO_2: Review of atmospheric CO_2 exchange in urban environments measured by eddy covariance technique. *Geography Compass* 4/9: 1238–1259.

Vesala T., Järvi L., Launiainen S., Sogachev A., Rannik Ü., Mammarella I., Siivola E., Keronen P., Rinne J., Riikonen A. & Nikinmaa E. 2008. Surface–atmosphere interactions over complex urban terrain in Helsinki, Finland. *Tellus* 60B: 188–199.

Vogt M., Nilsson E.D., Ahlm L., Mårtensson E.M. & Johansson C. 2011. The relationship between 0.25–2.5 μm aerosol and CO_2 emissions over a city. *Atmos. Chem. Phys*. 11: 4851–4859.

Wienhold F.G., Frahm H. & Harris G.W. 1994. Measurements of N_2O fluxes from fertilized grassland using a fast-response tunable diode-laser spectrometer. *J. Geophys. Res. Atmos*. 99: 16557–16567.

Wienhold, F.G., Welling, M. & Harris G.W. 1995. Micrometeorological measurement and source region analysis of nitrous-oxide fluxes from an agricultural soil. *Atmos. Environ*. 29: 2219–2227.